Seasonal time-course of gradients of photosynthetic capacity and mesophyll conductance to CO2 across a beech (Fagus sylvatica L.) canopy

Pierre Montpied, André A. Granier, Erwin Dreyer

Journal of Experimental Botany, Vol. 60, No. 8, pp. 2407–2418, 2009
doi:10.1093/jxb/erp093

Journal of Experimental Botany
www.jxb.oxfordjournals.org

RESEARCH PAPER

Seasonal time-course of gradients of photosynthetic capacity and mesophyll conductance to CO_2 across a beech (*Fagus sylvatica* L.) canopy

Pierre Montpied[1,2,*], André Granier[1,2] and Erwin Dreyer[1,2,*]

[1] INRA, UMR 1137, Ecologie et Ecophysiologie Forestières, F-54280 Champenoux, France
[2] Nancy-Université, UMR 1137, Ecologie et Ecophysiologie Forestières, F-54500 Vandoeuvre les Nancy, France

Received and Revised 26 November 2008; Accepted 25 February 2009

Abstract

Leaf photosynthesis is known to acclimate to the actual irradiance received by the different layers of a canopy. This acclimation is usually described in terms of changes in leaf structure, and in photosynthetic capacity. Photosynthetic capacity is likely to be affected by mesophyll conductance to CO_2 which has seldom been assessed in tree species, and whose plasticity in response to local irradiance is still poorly known. Structural [N and chlorophyll content, leaf mass to area ratio (LMA)] and functional leaf traits [maximum carboxylation rate (V_{cmax}), maximum light-driven electron flux (J_{max}), and mesophyll conductance (g_i)] were assessed by measuring leaf response curves of net CO_2 assimilation versus intercellular CO_2 partial pressure, along a vertical profile across a beech canopy, and by fitting a version of the Farquhar model including g_i. The measurements were repeated five times during a growth season to catch potential seasonal variation. Irradiance gradients resulted in large decreasing gradients of LMA, g_i, V_{cmax}, and J_{max}. Relative allocation of leaf N to the different photosynthetic processes was only slightly affected by local irradiance. Seasonal changes after leaf expansion and before induction of leaf senescence were only minor. Structural equation modelling confirmed that LMA was the main driving force for changes in photosynthetic traits, with only a minor contribution of leaf Nitrogen content. In conclusion, mesophyll conductance to CO_2 displays a large plasticity that scales with photosynthetic capacity across a tree canopy, and that it is only moderately (if at all) affected by seasonal changes in the absence of significant soil water depletion.

Key words: Canopy, European beech, irradiance, leaf structure, LMA, mesophyll conductance, photosynthetic capacity, plasticity.

Introduction

During the last decades, the increase of atmospheric CO_2 concentration and its consequences on climate have promoted a growing interest in the function of forest ecosystems as potential carbon sinks. This has led to the development of a number of functional models aiming at predicting the future role and importance of forests in carbon assimilation and storage. One of the key steps in these models is the estimation of carbon assimilation by leaves and its integration to canopy scale by considering the vertical gradients of environmental variables and of leaf photosynthetic capacities within canopies (Baldocchi and Harley, 1995; Chen *et al.*, 1999). Most of them use the model of Farquhar *et al.* (1980) for estimating leaf photosynthesis, as this approach has the advantage of including leaf photosynthetic capacity as described by the maximal carboxylation rate (V_{cmax}) and maximal light-driven electron flux (J_{max}). Photosynthetic capacity is independent of instantaneous climate fluctuations, expresses potential rather than actual photosynthesis, and is plastic, i.e. may change with micro-climate over days or weeks. Recently, several studies have pointed out the need to include seasonal variations of leaf photosynthetic capacity

* To whom correspondence should be addressed. E-mail: montpied@nancy.inra.fr or dreyer@nancy.inra.fr

in such models (Wilson *et al.*, 2000, 2001; Wang *et al.*, 2003; Muraoka and Koizumi, 2005; Kosugi and Matsuo, 2006). These studies, however, focused on sun leaves or simply distinguished between shade and sun leaves but did not take into account the vertical irradiance gradient as a continuum under which plasticity of leaf structure and photosynthetic capacity is expressed, nor did they consider potential seasonal changes of leaf traits along the gradient.

They also investigated only apparent values of the parameters (J_{max} and, if not only, V_{cmax}) of the model of Farquhar *et al.* (1980). Indeed, these parameters are usually derived from curves of net CO_2 assimilation rate (A) versus intercellular (C_i) and not chloroplastic CO_2 partial pressure (C_c). In other words, they assume that mesophyll conductance (g_i) to CO_2 is infinite. The use of apparent values of V_{cmax} and J_{max} is not problematic when the aim is to predict net CO_2 assimilation rates. It might be a serious drawback when analysing photosynthetic capacity in relation to leaf nitrogen (Ethier and Livingston, 2004) as apparent photosynthetic capacity and especially apparent V_{cmax} are largely underestimated compared with their actual values. Recent investigations revealed that g_i was smaller in shade than in sun leaves (Piel *et al.*, 2002; Flexas *et al.*, 2008). Further, low g_i might severely limit the rate of actual net CO_2 assimilation rate (A). The gradient of g_i, if any, and its seasonal variations therefore need be documented.

There are basically three techniques to estimate g_i: online $^{13}CO_2$ discrimination (Evans *et al.*, 1986), coupled measurements of chlorophyll fluorescence and gas exchange (Di Marco *et al.*, 1990; Loreto *et al.*, 1992), and derivation from A–C_i curves (Ethier and Livingston, 2004). A detailed account of these techniques can be found in Warren (2006). The first two techniques require complex measurements that might be difficult to deploy under field conditions, while the third one only requires accurate measurements of A–C_i relationships from which actual V_{cmax}, J_{max}, and g_i can be derived.

Another important issue for our understanding of the extent and seasonal variation of the photosynthesis gradient in forest canopies is to identify the primary driver for the plastic response of photosynthetic capacity to local irradiance. Irradiance-elicited plasticity of leaf traits has been the subject of a large number of investigations (Ellsworth and Reich, 1993; Niinemets and Tenhunen, 1997; Davi *et al.*, 2008), and a general result was that decreased irradiance resulted in decreased leaf mass to area ratio (LMA), decreased leaf thickness (fewer layers of palisade parenchyma cells), almost constant nitrogen content, and increased chlorophyll content on a mass basis. The main question therefore is to check whether the observed plasticity in photosynthesis (as described by V_{cmax}, J_{max}, g_i, and chlorophyll content) is directly driven by changes in LMA, by changes in N_{mass} (nitrogen content on a mass basis), or by changes in the relative allocation of nitrogen to photosynthesis. This question may be addressed using path analysis (Shipley, 2000).

The objectives of this study were to answer the following questions. (i) Is the irradiance-induced gradient of photosynthetic capacity paralleled by a gradient in mesophyll conductance to CO_2 (g_i) across a beech canopy? (ii) Is there a seasonal variation of photosynthetic capacity and of the irradiance-induced gradient across the canopy? (iii) Is the LMA the primary driving force for the plastic responses of photosynthesis across the canopy?

To answer these questions, A–C_i responses curves were recorded *in situ*, on leaves across a beech canopy at Hesse, Eastern France. A detailed version (Ethier and Livingston, 2004) of the Farquhar *et al.*, (1980) model was fitted to these curves to derive actual values of V_{cmax}, J_{max}, and g_i. Measurements were repeated five times during the growth season (from June to October). All data were adjusted to a common temperature of 25 °C from earlier estimates of temperature responses of the three parameters recorded on beech seedlings in a climate chamber (Dreyer *et al.*, 2001).

Materials and methods

Site

Measurements were made in a beech stand at Hesse, North Eastern France (48°40′N, 7°04′E, 305 m a.s.l.). The site is located amidst a 65 ha homogenous stand of 35-year-old beech trees. Tree density was ~3000 trees ha^{-1} and dominant tree height ~17 m. Mean annual (1974–2003) precipitation is 860 mm and mean annual temperature is 9.3 °C (Longdoz *et al.*, 2008). During 2001, annual precipitation was 1145 mm and rain events were evenly distributed all year round including summer (Fig. 1B); temperatures >30 °C occurred during only 4 d in August with an absolute maximum of 31.6 °C (Fig. 1C). Owing to these mild conditions, only a short and slight drought episode, i.e. with relative extractable soil water content (REW) <0.4, occurred between 12 August and 5 September (DOY 224–248; Fig. 1D). According to the course of relative global irradiance on the ground (Fig. 1A), the leaf area index (LAI) reached its maximum on 18 May and remained stable until the beginning of leaf shedding on 20 October.

Sampling

A scaffolding tower with floors every 2 m provided access to the canopy of ~10 trees. Five measurement campaigns were run during summer 2001 on the following dates: 19–22 June, 17–20 July, 7–10 August, 28–30 August, 4–5 October, referred to in the following as Jun, Jul, Aug1, Aug2, and Oct, respectively. Each campaign consisted of establishing a full net CO_2 assimilation rate—intercellular CO_2 partial pressure (A–C_i) response curve on about 3–4 leaves per floor in the tower. As a result each campaign provided 21 curves (18 during October).

Gas exchange measurements

Leaf gas exchange was measured with two inter-calibrated portable gas exchange systems Li6400 (LiCor, Lincoln, NE, USA) with a 2×3 cm leaf chamber and a red–blue diode

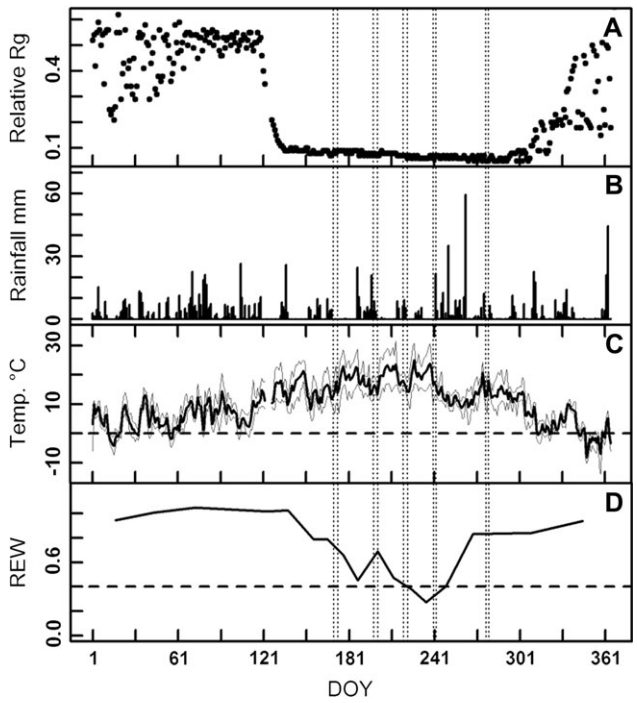

Fig. 1. Seasonal course of local climate during 2001. (A) Ratio of global irradiance at 1 m above the ground to global irradiance above the canopy. (B) Rainfall events (mm). (C) Daily mean (bold line), minimum and maximum (thin lines) air temperatures (°C); the dashed horizontal line=0°C. (D) Relative extractable soil water content; the dashed horizontal line represents the threshold (0.4) below which drought stress occurs. Vertical dotted lines indicate dates of measurement campaigns.

illuminator. Conditions in the chamber were set at 25 °C (except when ambient temperature was either too high or too low; see below for standardization procedures), photosynthetic photon flux density (PPFD) at 1000 μmol m^{-2} s^{-1} (for shade leaves) or 1500 μmol m^{-2} s^{-1} (sun leaves). Each response curve was preceded by at least 30 min activation under 20 Pa CO_2 and the target PPFD to induce full stomatal opening and photosynthesis activation. After full activation, CO_2 partial pressure in the chamber (C_a) was adjusted stepwise at 180, 150, 125, 100, 75, 50, 40, 30, 20, 15, 10, and 5 Pa (1 Pa≈10 vpm). Each step comprised 3 min for adjustment and stabilization followed by three data logs at 30 s intervals.

Leaves were then severed and chlorophyll content was recorded with a Minolta SPAD 502 chlorophyll-meter (Minolta Cameras Ltd, Japan). Leaves were then brought to the laboratory where leaf area was recorded with a DeltaT area meter (DeltaT Devices, Burwell, UK), and then they were dried during 48 h at 65 °C, weighed, and ground for N analysis with a CNS elemental analyser NCS2500 (CE Instruments, Thermo Quest, Italy). The following variables were computed for each leaf: LMA (g m^{-2}), N_{mass} (g kg^{-1}), and chlorophyll content (SPAD units). LMA was used as a surrogate for the irradiance received by leaves during their growth (Niinemets and Tenhunen, 1997).

Parameter estimation

A–C_i curves were fitted according to the widely used model of Farquhar and von Caemmerer (Farquhar *et al.*, 1980) modified according to von Caemmerer (2000) and Ethier and Livingston (2004) to compute maximal carboxylation rate (V_{cmax}), maximal light-driven electron flux (J_{max}), and dark respiration (R_d), and to take into account the mesophyll conductance to CO_2 (g_i). The V_{cmax} and J_{max} estimates provided here are therefore based on chloroplastic CO_2 partial pressure (C_c) and not on C_i, in contrast to many published data. The general model has been described in numerous papers and the version used here can be found in Ethier *et al*, (2006). The parameter set provided by Ethier *et al.* (2006) was used and the model was fitted jointly to the Rubisco-limited and the RuBP-limited segments of the A–C_i curves as described in Dreyer *et al.* (2001) and in Dubois *et al.* (2007). The estimated parameters V_{cmax}, J_{max}, g_i, and R_d were obtained from non-linear least-squares regression by means of the *nls* function from the R 2.5.1 software. (R-Development-Core-Team, 2007). As outlined by Warren and Adams (2006), estimating g_i from A–C_i curves might be delicate, and high quality data are required (Pons *et al.*, 2009). If these conditions are fulfilled, such estimates of g_i are in agreement with independent measurements such as combined gas exchange–chlorophyll *a* fluorescence measurements (Niinemets *et al.*, 2006; Warren and Dreyer, 2006). A–C_i curves that were noisy (for most of them, convergence problems occurred during the fit) were therefore discarded, and the remainder were kept when the standard error of the g_i estimate was <50% of the estimated value. A total of 73 A–C_i curves were finally retained among 97. R_d estimates based on A–C_i curves were not considered reliable because of high standard errors and are not analysed further.

Temperature corrections

Most A–C_i curves were measured at 25 °C leaf temperature, but in some cases external temperatures were too low to allow measurements at 25 °C. In such cases, the parameters of interest (g_i, V_{cmax}, and J_{max}) were standardized later on to their value at 25 °C. To establish the parameters for the temperature response of the three variables, the data set published by Dreyer *et al.* (2001) for beech seedlings under a range of leaf temperatures was used. The A–C_i response curves (five different leaves under the different levels of temperature) were fitted with the above-described procedure to obtain estimates of g_i, V_{cmax}, and J_{max} of the same leaves at 10, 18, 25, 32, 36, and 40 °C, with five different leaves. These data were then fitted to two temperature response models.

(i) The Arrhenius function when the parameter increased monotonously with temperature (Leuning, 1997):

$$P(T) = P(T_{ref}) \times e^{\frac{\Delta H_a}{RT_{ref}}\left(1-\frac{T_{ref}}{T}\right)} \quad (1)$$

where $P(T)$ is the value of the parameter at leaf temperature T (K), $P(T_{ref})$ is the value of the parameter at reference

temperature T_{ref} (298.15 K), ΔH_a (kJ mol^{-1}) is the activation energy of the given parameter, and R is the gas constant (8.314 J K^{-1} mol^{-1});

(ii) The simplified model of June *et al.* (2004) when there was evidence of a maximum, i.e. an optimum, in temperature response:

$$P(t) = P(t_{opt}) \times e^{-\frac{(t-t_{opt})^2}{\Omega^2}} \quad (2)$$

where $P(t)$ is the value of the parameter at leaf temperature t (°C), $P(t_{opt})$ is the value at the optimal temperature t_{opt} (°C), and Ω (°C) is an adjustment parameter.

The fitting procedure was similar to the one used by Dreyer *et al.* (2001), i.e. the temperature response parameters were considered to be common to all leaves while the values of g_i, V_{cmax}, and J_{max} at 25 °C were assumed to be variable. The overall quality of those A–C_i curves was satisfactory and all were retained. Estimates were weighted by the reciprocal of their squared standard error (Murtaugh, 2007) to minimize the influence of poorly estimated parameters.

Statistics

The statistical analyses were performed as covariance analyses of the effect of the measurement campaigns (date effect) with LMA (surrogate of the irradiance received by the leaves) as covariate, using the R software (R-Development-Core-Team, 2007).

The general approach was first to fit a main model of the form:

$$R_{ir} = a_i + b_i \cdot LMA_{ir} + \varepsilon_{tr} \quad (3)$$

or:

$$R_{ir} = a_i \cdot LMA_{ir}^{bi} + \varepsilon_{tr} \quad (4)$$

with indices i referring to date number, r to replicates; parameters a_i, intercept (model 3) or scaling parameter (model 4) at date i; b_i slope (model 3) or exponent (model 4) at date i; R_{ir}, response; and ϵ_{ir}, error term. The choice between the linear model (3) and the power law model (4) was based on an analysis of the residuals against predicted plots that should show a horizontal tendency. When the response variate was an estimate from a fitting procedure, such as V_{cmax}, J_{max}, and g_i from A–C_i curves, it was weighed by $1/SE^2$, with SE the standard error of the estimate. Then a cascade of nested models were fitted by setting to zero or equalizing the parameters that were not significantly different ($P < 0.05$) from zero or not significantly different among each other. Slope or exponent parameters were checked first. At the end of the procedure, the most parsimonious (i.e. with the lowest number of parameters) model that was not significantly different (F-test between main and submodel) from the main model was retained. At this stage, and if required, multiple comparison tests using the multivariate t distributions of the parameters were performed on parameters of interest with the *multcomp* R-package (Hothorn *et al.*, 2007). Only the results of this final model will be detailed in the text. Normality and homoscedasticity were checked graphically by plotting residuals against predicted and by normal quantile to quantile plots. When heteroscedastity was eventually evidenced, the residual variance was modelled as a power function of predicted.

Results

Temperature responses of g_i, V_{cmax}, and J_{max} of beech saplings (Fig. 2)

The temperature response of V_{cmax} was monotonously increasing without inflexion within the experimental temperature range (Fig. 2A) and was therefore fitted with the simple Arrhenius model (Equation 1, Table 1). Temperature responses of J_{max} and g_i presented a maximum (Fig. 1B, C) estimated as 39.9±2.2 °C (mean±SE) and 26.9±0.6 °C, respectively, from the June model (Equation 2, Table 1). The three adjusted models were thereafter used to standardize all data at 25 °C.

Responses of LMA to height and date (Fig. 3)

The range of LMA values across the canopy was very large, from ~25 at the bottom to almost 120 g m^{-2} at the top of the canopy. The two-way analysis of variance (ANOVA) of LMA against height and date, and their interaction was compared with its nested one-way ANOVA against height only. LMA was log-transformed to homogenize variances. This comparison showed a lack of effect of date on LMA (n=73, df=22 and 45, F=1.138, P=0.347). LMA was under tight control of height (n=73, df=5 and 67, F=336, P <0.0001), i.e. of the irradiance gradient in the canopy. The seasonal stability of LMA, its tight correlation with height in the canopy, and previous studies on the same site showing a tight linear relationship (R^2 >0.95) between LMA and relative PPFD (not shown) justified the use of LMA as a surrogate of the irradiance load received by the leaves (Niinemets and Tenhunen, 1997).

Nitrogen content in leaves (N_{mass}) (Fig. 4)

N_{mass} was very close to 20 g kg^{-1} in all leaves and canopy positions. The linear relationship (Equation 3) between LMA and N_{mass} at the different dates is shown in Fig. 4. The most parsimonious model (n=73, df=67, R^2=0.382) that did not differ significantly from the main model (3) (F=1.18, df=4 and 63, P=0.330) showed that there was a small but significant negative slope of the relationship, common to all dates, and that the intercept ranking of the dates was: Aug1^a>Jul^a>Aug2^{ab}>Oct^b>Jun^b [levels sharing the same letter are not significantly different ($P \geqslant 0.05$)]. N_{mass} increased slightly in all leaves independently from LMA (i.e. from the canopy layer) from June to July then stabilized during summer before declining again during senescence in October (inset, Fig. 4).

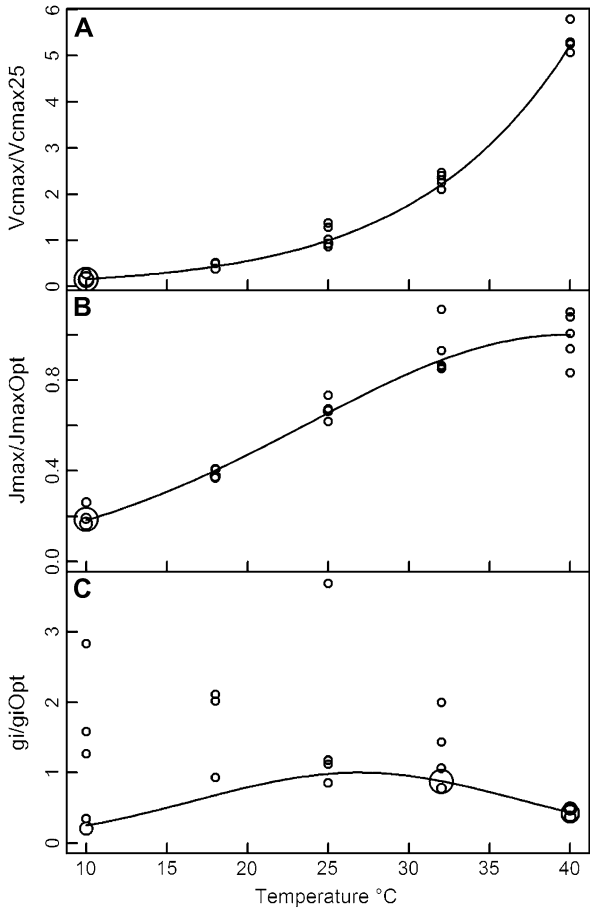

Fig. 2. Temperature responses of photosynthetic parameters. (A) Ratio of V_{cmax} to V_{cmax} at the reference temperature (25 °C) (Arrhenius model); (B) ratio of J_{max} to J_{max} at the optimum temperature (June model); (C) ratio of g_i to g_i at the optimum temperature (June model). The diameter of the symbols is linearly related to their weight (reciprocal of their estimation variances).

Table 1. Parameter estimates (SE) of Arrhenius and June temperature response models for V_{cmax}, J_{max}, and g_i

	V_{cmax}	J_{max}	g_i
ΔH_a (Arrhenius) (kJ mol^{-1} K^{-1})	85.6 (2.8)	–	–
T_{opt} (June) (°C)	–	39.9 (2.2)	26.9 (0.6)
Ω (June) (dimensionless)	–	22.9 (1.5)	14.3 (0.9)

Estimates of chlorophyll content per leaf area (SPAD units) (Fig. 5)

Chlorophyll content per leaf area as detected by SPAD units was linked to LMA by a power function (Equation 4). Residual variance increased with predicted and was therefore modelled as a power function of predicted. The most parsimonious model (n=69, df=63, R^2=0.647) that did not differ significantly from the main model (F= 0.921, df=4 and 59, P=0.458) revealed that there was a slight but significant and positive exponent between LMA and SPAD. The exponent was stable with dates, and

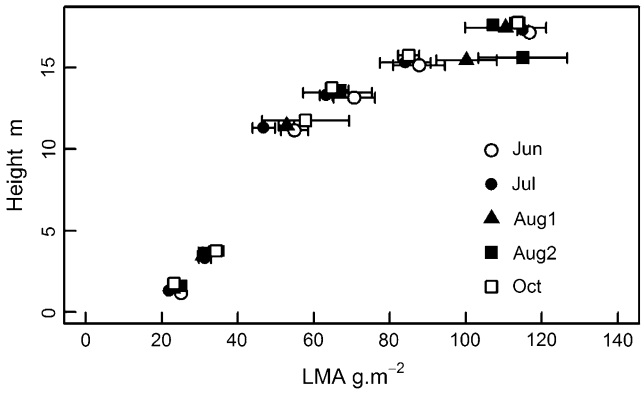

Fig. 3. Relationship between leaf mass to area ratio (LMA, g m^{-2}) and height (m) in the canopy. Error bars show standard errors.

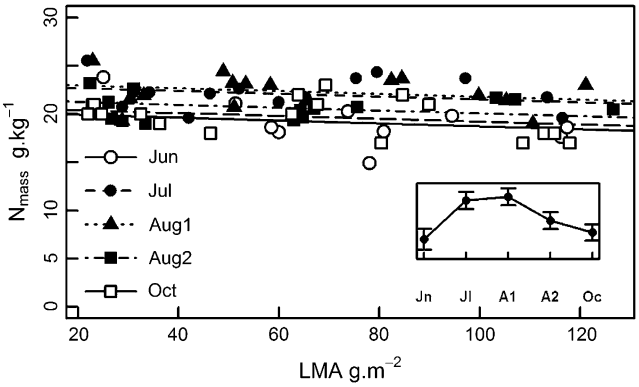

Fig. 4. Leaf nitrogen content on a mass basis (g kg^{-1}) versus LMA. Regression lines per date represent the fitted model (see text). Inset: seasonal time course of the intercept of regression lines.

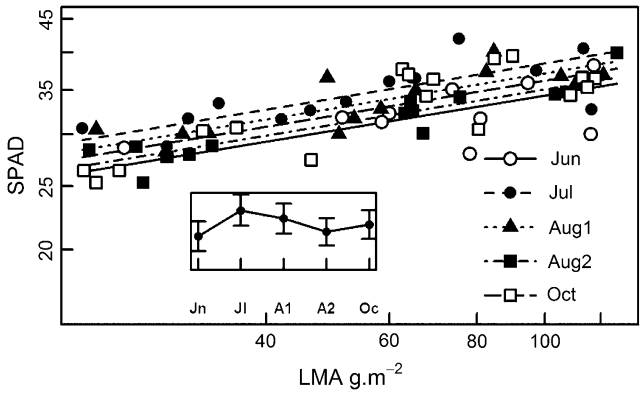

Fig. 5. Leaf SPAD units versus LMA. Log-scale on the *x*- and *y*-axes. Regression lines per date represent the fitted model (see text). Inset: seasonal time course of the intercept of regression lines.

the scaling parameter ranked as follows: Jul^{a}>Aug1^{ab}> Oct^{b}>Aug2^{b}>Jun^{b} [levels sharing same letter are not significantly different ($P \geqslant 0.05$)]. In other words, there was a seasonal dynamics in SPAD units with a small increase during early summer and a decrease during late summer (inset, Fig. 5). The changes remained moderate.

Maximal carboxylation rate (V_{cmax}) (Fig. 6A)

V_{cmax} displayed a large range of values from 10 μmol m^{-2} s^{-1} to >100 μmol m^{-2} s^{-1}. The most parsimonious power law model (Equation 4, n=73, df=67, R^2=0.827, weighted R^2=0.934) that did not differ from the main model (F=1.61, df=4 and 63, P=0.182) revealed a tight relationship and positive gradient between V_{cmax} and LMA. This relationship was not significantly different between the three mid-summer dates July, early August, and late August. The gradient was significantly lower during the June campaign whereas it was steeper in October. V_{cmax} values at similar LMA were also lower in October compared with mid-summer.

Maximal light-driven electron flux (J_{max}) (Fig. 6B)

J_{max} displayed a large variability parallel to that of V_{cmax} and ranging from 10 μmol m^{-2} s^{-1} to almost 200 μmol m^{-2} s^{-1} and was tightly related to LMA. The most parsimonious power law model (Equation 4, n=73, df=67, R^2=0.921, weighted R^2=0.941) that did not differ significantly from the main model (F=1.79 df = 4 and 63, P=0.143) revealed a common exponent for all dates. The scaling parameter ranked as follows: $Aug2^{a}$<Jun^{ab}<$Aug1^{bc}$<Oct^{c}<Jul^{c} [levels sharing the same letter are not significantly different ($P \geqslant 0.05$)]. Despite these significant differences, the five dates yielded very close values of J_{max}, and the time course showed an increase from June to July then a decrease until late August and then again an increase until October (inset, Fig. 6B).

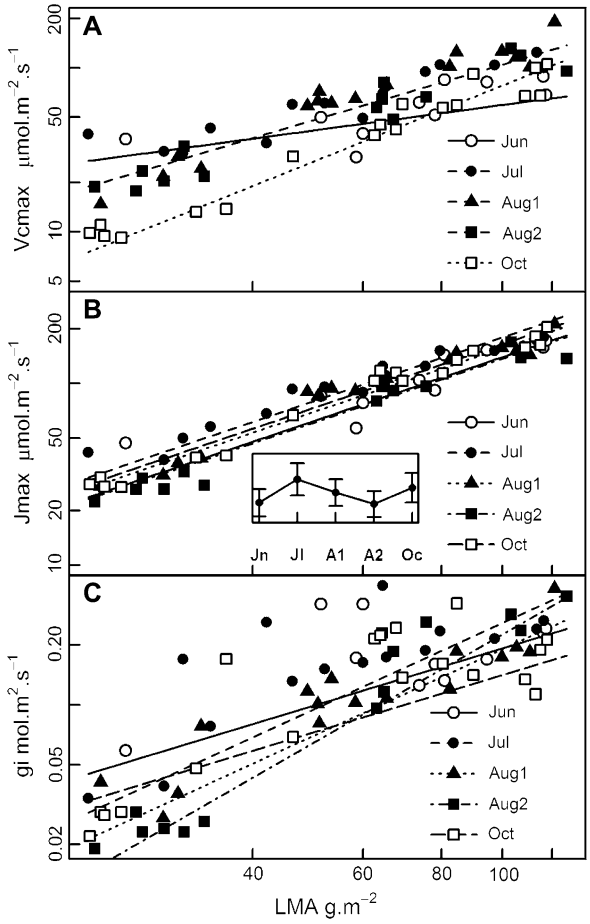

Fig. 6. Leaf photosynthetic parameters at 25 °C versus LMA. Log-scale on the *x*- and *y*-axes. (A) Maximal carboxylation rate at 25 °C (V_{cmax}, μmol m^{-2} s^{-1}); (B) maximal light-driven electron flux at 25 °C (J_{max}, μmol.m^{-2}.s^{-1}); (C) mesophyll conductance to CO_2 at 25 °C (g_i, mol m^{-2} s^{-1}). Regression lines per date represent the fitted model (see text). Inset: seasonal time course of the intercept of regression lines for J_{max}.

Mesophyll conductance to CO_2 transfer (g_i) (Fig. 6C)

Despite a larger data scatter than for V_{cmax} and J_{max}, g_i clearly increased with LMA. Values ranged from 0.02 mol m^{-2} s^{-1} to 0.40 mol m^{-2} s^{-1}. The most parsimonious power law model (Equation 4, n=73, df=65, R^2=0.515, weighted R^2=0.898) that was not significantly different from the main model (F=0.692, df=2 and 63, P=0.504) led to the following conclusions: the exponent, i.e. the gradient in the canopy, was always significantly different from 0 and positive, but was lowest in June and October, largest in late August, and intermediate in July and early August. In October, g_i was lower than on the other dates in the upper canopy but similar in the lower layers.

Relative nitrogen allocation to V_{cmax} and J_{max} (Fig. 7)

Relative allocation of leaf nitrogen to carboxylation (P_c) and to light-driven electron flow (P_b) was calculated according to Niinemets and Tenhunen (1997).

P_c was linearly related to log(LMA); and a linear model (Equation 3) was fitted to log(LMA). Examination of residuals revealed that variance was increasing with

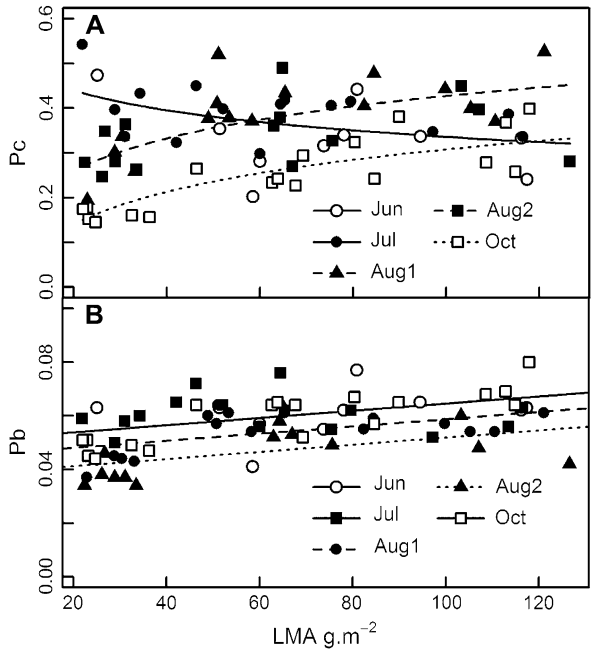

Fig. 7. Nitrogen allocation to carboxylation (P_c) and to light-driven electron flow (P_b) calculated according to Niinemets and Tenhunen (1997) versus LMA. Regression lines per date represent the fitted model (see text).

predicted; therefore, variance was modelled as a power function of predicted. The most parsimonious model (n=73, df=68, R^2=0.576) that was not significantly different from the main model (F=1.78, df=5 and 63, P=0.131) revealed (Fig. 7A) that the gradient of P_c against LMA was positive during early summer (June and July), but was reversed afterwards. The gradient remained stable from early August to October, but a downward shift of P_c occurred between late August and October.

P_b was linearly related to LMA, and the most parsimonious model (Equation 3, n=73, df = 69, R^2=0.983) that was not significantly different from the main model (F=1.77, df = 6 and 63, P=0.120) revealed (Fig. 7B) a constant and positive gradient of P_b against LMA. Nevertheless, the intercept differed significantly and was ranked as follows: $Aug2^a<Aug1^b<Jun^c=Jul^c=Oct^c$ [levels sharing the same letter are not significantly different ($P \geqslant 0.05$)].

Nitrogen allocation to chlorophylls (Fig. 8)

Nitrogen allocation to chlorophylls was analysed based on the ratio of SPAD units to nitrogen per unit area (N_{area}) as a surrogate. The relationship between this ratio and LMA obeyed a power function and was fitted to Equation 4, and residual variance modelled as a power function of predicted. The most parsimonious model (n=69, df=63, R^2=0.973) that was not significantly different from the main model (F=1.631, df=4 and 59, P=0.178) revealed an exponent common to all dates, but a significantly different scaling parameter between dates, that were ranked as follows (inset, Fig. 8): $Aug1^a<Aug2^a<Jul^{ab}<Jun^{ab}<Oct^b$ [levels sharing the same letter are not significantly different ($P \geqslant 0.05$)]. However, absolute differences between these parameters remained very small.

Discussion

Quality and reliability of photosynthetic parameter estimation

Jointly estimating the four parameters V_{cmax}, J_{max}, g_i, and R_d from A–C_i curves is technically difficult and may lead to erroneous estimates or large standard errors of the estimation (Dubois *et al.*, 2007) unless data quality is carefully checked. For this reason, some A–C_i curves that displayed a large data scatter were discarded and all further analyses were performed by weighting the estimated parameters by the reciprocal of their quality measured by the variance of their estimation. This ensured that poorly estimated parameters did not influence the analyses too severely.

Ethier and Livingston (2004) showed that assuming an infinite mesophyll conductance leads to a large underestimation of V_{cmax} and to a lesser extent of J_{max}. In the present study, g_i was assumed to remain constant during the establishment of each A–C_i curve. It was recently evidenced that g_i might change rapidly under a changing microenvironment and particularly with varying C_i (Flexas *et al.*, 2007, 2008) but this point is still controversial (Tazoe *et al.*, 2009). No model of g_i response to C_i has yet been proposed and it is therefore impossible to integrate short-term changes of g_i into a procedure to estimate parameters of Farquhar's model. The compromise used in the present study produced estimates of photosynthetic capacity parameters closer to the 'true' values than to the 'apparent' values as derived from a fit to the original version of the model. g_i estimates produced here may therefore be interpreted as a 'mean' mesophyll conductance over the range of CO_2 partial pressure values used during the establishment of the curves.

Temperature responses

The estimated thermal optimum of g_i was 26.9±0.6 °C and agrees with earlier findings of Warren and Dreyer (2006) and Yamori *et al.* (2006). The peak observed in the temperature response of apparent V_{cmax}, when estimated assuming infinite g_i (Dreyer *et al.*, 2001), disappeared when V_{cmax} was estimated on a C_c basis like in the observations by Warren and Dreyer (2006). J_{max}, however, still peaked close to 40 °C, as its estimate is only moderately influenced by g_i. The use of this information helped scale all results to a common temperature of 25 °C, which is a prerequisite for the anlaysis of plastic responses to irradiance and to seasonal changes of photosynthetic properties.

Gradients in the canopy

Leafs traits related to photosynthesis are well known to display large gradients across canopies, due mainly to the intracanopy gradient of local irradiance. LMA is known to respond severely to relative irradiance, either linearly (Niinemets, 1995; Niinemets and Tenhunen, 1997) or logarithmically (Iio *et al.*, 2005; Utsugi *et al.*, 2005). In the latter cases, the discrepancy from the linear response was mainly induced by the lowest levels of relative irradiance. The observed relationship between LMA and height was stable in time, as found by Wilson *et al.* (2000) and Utsugi *et al.* (2005), at least in the time interval between full leaf expansion and the start of senescence. Moreover, a linear relationship was found between LMA and relative irradiance during earlier measurements in the beech canopy at

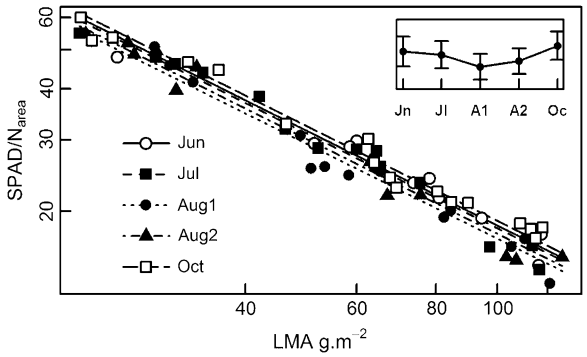

Fig. 8. Ratio of SPAD readings to nitrogen on an area basis (SPAD/N_{area}, SPAD units m^2 g^{-1}) versus LMA. Log-scale on the x- and y-axes. Regression lines per date represent the fitted model (see text). Inset: seasonal time course of the intercept of regression lines.

Hesse. These observations confirmed that the use of LMA as a surrogate for relative irradiance was a valid simplifying choice (Niinemets, 1995; Niinemets and Tenhunen, 1997).

N_{mass} displayed a very small gradient across the canopy (<10% between extremes): this gradient might be due to a dilution effect by non-structural carbohydrates (NSCs) in leaves (Niinemets, 1995), to thicker cell walls that display low N content (Roderick *et al.*, 1999; Shipley *et al.*, 2006), or to a greater relative biomass of veins and petioles in sun leaves. These findings are consistent with the literature that reports a lack of gradient (Ellsworth and Reich, 1993) or a weakly negative one (Niinemets, 1995; Iio *et al.*, 2005) for broad-leaved canopies. As a result, N_{area} paralleled tightly the gradient of LMA across the canopy.

SPAD readings are closely correlated to chlorophyll content per leaf area (Richardson *et al.*, 2002; van den Berg and Perkins, 2004). However, the relationship between chlorophyll meter readings and chlorophyll content might change with environmental conditions such as irradiance or leaf water status (Martinez and Guiamet, 2004). In the present study, the relationship between LMA and the ratio of SPAD readings to N_{area} was almost perfectly stable throughout the growing season. On the other hand, leaves did not experience any real drought stress during the 2001 summer. One can therefore be rather confident that SPAD units can be safely used as a surrogate of chlorophyll content throughout the growing season.

The observed gradient of chlorophyll content, i.e. larger chlorophyll content on an area basis in sun leaves compared with shade leaves, agrees with the observations made by Demarez *et al.* (1999) in a comparable beech canopy but contradicts the findings of Lichtenthaler *et al.* (2007) and Iio *et al.* (2005). However, the latter studies were performed with only the dominant trees and excluded suppressed trees. The present study included leaves from the latter that display very small values of LMA and SPAD and therefore expanded the range of values available across the whole canopy.

Photosynthetic capacity as described by the parameters V_{cmax}, J_{max}, and g_i displayed a steep vertical gradient across the canopy. This is now a well-established feature for apparent V_{cmax} and J_{max} (Ellsworth and Reich, 1993; Niinemets and Tenhunen, 1997; Meir *et al.*, 2002). Nevertheless, vertical profiles of g_i were to date never characterized whereas g_i is known to be usually smaller in shade than in sun leaves (Hanba *et al.*, 2002; Piel *et al.*, 2002; Flexas *et al.*, 2008). This confirms the occurrence of a tight coordination between the three parameters describing leaf photosynthesis, V_{cmax}, J_{max}, and g_i, that display similar and parallel variations across the canopy, i.e. similar irradiance-elicited plasticity.

If stomatal density were constant in relation to local irradiance, the path length of passive diffusion of CO_2 from substomatal cavities to the carboxylation sites would be expected to be shorter in shade leaves that have fewer palisade parenchyma layers (Eschrich *et al.*, 1989) and therefore increased g_i. However, Aranda *et al.* (2003) have shown that stomatal density decreases with decreasing irradiance in *F. sylvatica* leaves which might counteract the effect of the increased number of palisade parenchyma layers on diffusion path length. However, structural leaf traits correlated with LMA such as mesophyll thickness or mesophyll cell surface area have also been shown to influence g_i positively (Terashima *et al.*, 2001). The vertical gradient of g_i might, therefore, be attributed, at least partly, to a structural plasticity of leaf anatomy as expressed by LMA. Nevertheless, it is known (Piel *et al.*, 2002) that the diffusion component is small, at least in broadleaved deciduous species (<20%) and that the liquid phase component plays a major role. A clear identification of the correlation between liquid phase conductance and cell structure and membrane constituents is still under discussion (Uehlein *et al.*, 2008).

The vertical gradient of relative allocation of nitrogen to carboxylation (P_c) or to bioenergetics (P_b) was weak (30–50% between extreme values) with respect to the gradients displayed by V_{cmax} and J_{max} (~5- to 6-fold), i.e. the changes in photosynthetic capacity across the canopy were not driven by changes in N_{mass} (see above) but mainly by leaf structure (LMA to a large extent) and to a lesser extent by the relative allocation of N to photosynthesis (P_c and P_b). The small gradient observed for P_c was negative during early summer and positive later on, while P_b displayed a small and positive gradient during the whole growth season.

In contrast, the gradient of nitrogen allocation to light capture, as indicated by the ratio of SPAD readings to N_{area}, was steep, ~4-fold, and negative (from low to high irradiance). The structural adjustments through LMA in response to irradiance described by Terashima *et al.* (2001) as a direct consequence of structural and physiological constraints on CO_2 diffusion inside the leaves are compensated through changes in nitrogen allocation to light capture, so as to maintain a large leaf absorbtance even in the lowest leaves with low LMA. However, a slight gradient of chlorophyll content per unit leaf area was still observed, suggesting that nitrogen shortage occurred in the lowest leaves present on suppressed trees.

Functional links between variables

The bivariate approach used for analysing the responses of the different variables to the irradiance gradient cannot differentiate between their direct and indirect relationships. A multivariate approach using path analysis with the d-sep method of Shipley (2000) was therefore used to disentangle the complex relationships between variables measured across the beech canopy. Analysis was performed on the covariance matrix of the log-transformed variables centred around their mean by date to take into account the structure of the data set (Shipley, 2000). Degrees of freedom were adjusted to total observation number (69) minus number of groups (five dates) to take into account centring of variables around date means. Four observations with missing data were excluded. Multinormality of the data set was checked with Mardia's test (Shipley, 2000). The approach of centring variables by their mean per measurement campaign implicitly assumes that seasonal variations were small, as discussed below, and had only little influence

on the detected functional relationships. This was confirmed by the fact that at least two path models were not rejected. The above discussion already suggested that LMA was the key variable controlling the overall irradiance-elicited plasticity in photosynthetic traits and that leaf nitrogen content (N_{mass}) only secondarily affected this plastic response. In a first step, these two variables were identified as the roots of the path models with, however, a functional link from LMA to N_{mass} accounting for the dilution effect of N_{mass} by LMA discussed above. In a second step, the other variables, all related to leaf photosynthetic capacity, were modelled as being controlled by LMA and N_{mass}. At this stage, several hypothetical paths could be postulated. A first model (Fig. 9, model 1) assumed that they were all controlled independently by LMA and N_{mass}. This model was clearly rejected (Fisher C test: χ^2=59.2, df=12, $P < 0.0001$), which indicates that some coordination occurs between these variables independently from the gradient of local irradiance. It has been outlined above that the chlorophyll content gradient is steeper when expressed on a leaf mass basis than on a leaf area basis and that it is the reverse for photosynthetic capacity (V_{cmax}, J_{max}, and g_i), suggesting that chlorophyll content behaves, with respect to the driving variables N_{mass} and LMA, independently of the other variables.

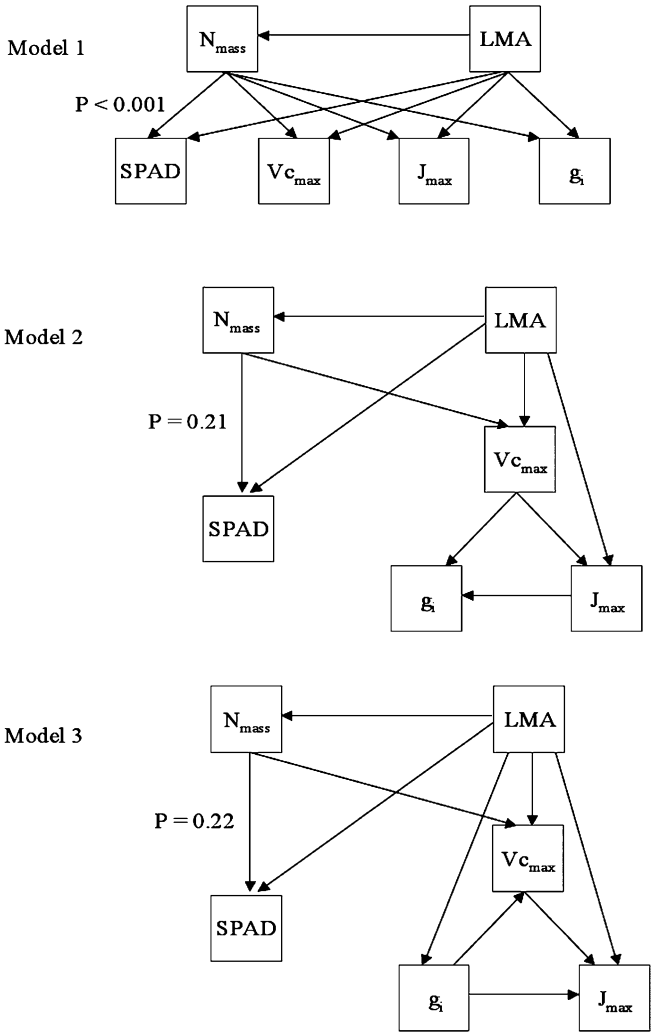

Fig. 9. Path models describing the functional relationships between LMA, N_{mass}, SPAD units (scaling to chlorophyll content on an area basis), V_{cmax}, J_{max}, and g_i. See text for discussion.

Therefore, several path models that assumed independence of chlorophyll content (SPAD) from photosynthetic capacity were tested. The current knowledge about the relationships between the latter variables does not allow any particular pathway relating them to be postulated, and therefore most of the models encompassing biologically sound relationships were fitted. Among these, only two (Fig. 9, models 2 and 3) were not rejected.

In model 2, LMA controls N_{mass}, and chlorophylls (SPAD) are controlled independently from the other photosynthesis parameters by LMA and N_{mass}. In addition, there is a coordination between V_{cmax}, J_{max}, and g_i in the leaves depending on nitrogen allocation: V_{cmax} is controlled by both LMA and N_{mass}, then V_{cmax} controls g_i and J_{max}, and J_{max} also controls g_i (if this last condition is not respected, then the model is rejected). LMA also controls J_{max} independently of the previous controls (i.e. nitrogen allocation to J_{max} relative to V_{cmax} is modified by irradiance). This model was not rejected (Fisher's C test: χ^2=15.6, df=12, P=0.210).

Model 3 is similar to model 2 but g_i acts as a control over V_{cmax} and J_{max}, and is controlled similarly by LMA (i.e. by irradiance). If the latter conditions are not respected, then the model is rejected. J_{max} is still controlled by V_{cmax} and LMA (i.e. by irradiance). This model was not rejected either (Fisher's C test: χ^2=13.1, df=10, P=0.220).

Several other models have been checked and the general conclusions were: when a direct control of V_{cmax} by N_{mass} was hypothesized, then including a direct control of g_i or J_{max} by N_{mass} led to rejection of the models; a direct control of V_{cmax} on J_{max} had to be included in addition to a direct control of LMA on J_{max}, otherwise the models were rejected. Interestingly, these models show that J_{max} is not solely determined by V_{cmax} but also and independently by LMA (i.e. by the irradiance gradient) too, invalidating the constancy of the ratio of J_{max} to V_{cmax}. The absence of paths linking nitrogen content to any other variable but V_{cmax} indicates that nitrogen content determines the overall pool of proteins involved in carbon fixation but that its level does not influence the balance in relative allocation to the different photosynthetic functions. Besides, these models show that there are functional links between g_i and photosynthetic capacity, and confirm the functional links between light-saturated assimilation and mesophyll conductance evidenced by Terashima *et al.* (2001) in a structural–functional modelling approach.

Seasonal variations

The climate throughout the 2001 growth season had remained mild, and only a short and slight drought episode occurred during late August. This might have affected the outcome of the late August measurement campaign (Aug2). However, no indication of severe drought stress was noticed

when A–C_i response curves were established: stomatal conductance and net assimilation (not shown) during the measurements were similar to those recorded during the other measurement campaigns. There are nevertheless some indications for mild stress effects during this campaign: mesophyll conductance of shade leaves was lower than during all other campaigns and relative nitrogen allocation to bioenergetics was at its lowest. However, if a stress actually occurred, it affected only understorey trees, which have a small if not negligible contribution to whole canopy carbon fixation. Morover, the decline in relative allocation of N to bioenergetics might simply be the continuation of the overall decrease observed from June to early August.

Once maximum values were reached in mid-May, 3–4 weeks before the first campaign, LAI remained stable until late October, 2 weeks after the last campaign. Similarly LMA was stable and, therefore, the only driving variable that may have changed during the course of the season is leaf nitrogen: its total amount could have been affected by reallocations either between leaves in the canopy, or between leaves and storage organs. Another change could have affected the relative allocation of N to the different photosynthetic processes. Total nitrogen amount in the canopy, as estimated from the intercept of the N_{mass} versus LMA relationship, varied slightly: it increased from June to mid-summer and then decreased until early October. The observed changes did not reveal major translocation processes. Furthermore, the nitrogen gradient (i.e. the slope of the N_{mass} versus LMA relationship) remained stable throughout the growth period, indicating that there was no noticeable nitrogen redistribution between the upper and lower canopy.

The only noticeable changes affected the relative allocation of nitrogen to the different photosynthetic processes at an intra-leaf scale. Relative allocation of N to light capture was very stable: the slope of the relationship between LMA and the ratio SPAD/N_{area} remained stable throughout the growing season and the small but significant seasonal trend in the intercept reversely followed that of N_{mass}. This latter fact indicates that the absolute amount of N invested into light capture remained stable throughout the season, as was also observed by Demarez *et al.* (1999).

Seasonal variations of V_{cmax} resulted mainly in smaller gradients and higher variability during early summer than during late summer and autumn. This advocates for a slow acclimation to changes in the irradiance gradient (Frak *et al.*, 2001) due to leaf emergence and expansion in spring. This is confirmed by the reversion of the gradient of relative N allocation to carboxylation observed between June and July and the following months. A general and important decrease of V_{cmax} and of nitrogen allocation to carboxylation was observed during the last October campaign, while N_{mass} decreases only weakly at that time. This suggests that autumn senescence was beginning and resulted in deactivation if not degradation of Rubisco.

Seasonal variations of the J_{max} profiles were less marked: the gradients remained the same throughout the growth season, and the seasonal course of the scaling parameter was similar to that of N_{mass} until the end of summer but not in October where J_{max} increased whereas N_{mass} decreased. This was confirmed by the evolution of the nitrogen allocation to bioenergetics (Fig. 7B). The increase of J_{max} and, in parallel, of nitrogen allocation to bioenergetics in October remained difficult to interpret.

Some changes occurred throughout the growth season in g_i gradients but these remained small compared with the large variablity of these data, and no sound interpretation could be elicited except for the g_i decrease in shade leaves in late August that was possibly attributed to the small drought stress occurring at that time, as discussed above.

Several studies reported a very visible seasonal time course of apparent V_{cmax} in sun leaves of broad-leaved deciduous forests and claimed the importance of considering the seasonal trends of photosynthetic capacity when modelling ecosystem carbon fluxes. However, no universal trend could be drawn from such results. Some report a peak in early summer followed by a slow decrease until the beginning of senescence when the decrease accelerates (Wilson *et al.*, 2000). Others evidenced a rapid increase in spring followed by a slow increase during summer before the autumnal, senescence-induced decrease (Muraoka and Koizumi, 2005) or a dome-like evolution peaking during mid-summer (Kosugi and Matsuo, 2006; Wang *et al.*, 2008). In the present study, there was no evidence of any time course of V_{cmax} in the upper leaves (LMA >80 g m^{-2}) during summer except an increase between the June and July campaigns and a decrease in early October. Many factors might be involved in these differences, such as species behaviour, site and climate effects, and occurrence and intensity of drought events. Severe decreases in photosynthetic capacity were reported in longer lived sun leaves of evergreen species; they mainly occurred during the second growth season (Katahata *et al.*, 2007). In fully annual broad-leaved species with rather short-lived leaves, this may not be the case This question still deserves further research.

Conclusions

This study confirmed the primary role of structural adjustment through the plastic response of LMA for the acclimation of leaves to the local irradiance in a canopy, whereas biochemical adjustments through relative nitrogen allocation remained marginal. A strong co-ordination was evidenced between V_{cmax}, J_{max}, and mesophyll conductance, and was only slightly modulated by local irradiance. The plastic relationships between these parameters deserves further attention. In the absence of severe drought stress during summer, photosynthetic capacity proved to be quite stable in summer after a leaf expansion phase and before autumn senescence. A steep vertical gradient of mesophyll conductance was evidenced and should be considered when using multi-layered model of carbon fluxes in forest ecosystems.

Acknowledgements

The help of Delphine Retzinger and Michèle Ridolfi during measurement campaigns is gratefully acknowledged, as well

as the contribution of Jacqueline Marchand in analysing carbon and nutrient contents. Funding for this study was provided by the European program Carboeuroflux (EVK2-1999-00229). Helpful discussions about g_i with B Genty (CNRS-CEA, Cadarache, France) and CR Warren (University of Sydney), and about path analysis with B Shipley are gratefully acknowledged.

References

Aranda I, Bergasa LF, Gil L, Pardos JA. 2001. Effects of relative irradiance on the leaf structure of Fagus sylvatica L. seedlings planted in the understory of a Pinus sylvestris L. stand after thinning. *Annals of Forest Science* **58,** 673–680.

Baldocchi DD, Harley PC. 1995. Scaling carbon dioxide and water vapor exchange from leaf to canopy in a deciduous forest. II. Model testing and application. *Plant, Cell and Environment* **18,** 1157–1173.

Chen JM, Liu J, Cihlar J, Goulden ML. 1999. Daily canopy photosynthesis model through temporal and spatial scaling for remote sensing applications. *Ecological Modelling* **124,** 99–119.

Davi H, Barbaroux C, Dufrene E, Francois C, Montpied P, Breda N, Badeck F. 2008. Modelling leaf mass per area in forest canopy as affected by prevailing radiation conditions. *Ecological Modelling* **211,** 339–349.

Demarez V, Gastellu-Etchegorry JP, Mougin E, Marty G, Proisy C, Dufrene E, Le Dantec V. 1999. Seasonal variation of leaf chlorophyll content of a temperate forest. Inversion of the PROSPECT model. *International Journal of Remote Sensing* **20,** 879–894.

Di Marco G, Manes F, Tricoli D, Vitale E. 1990. Fluorescence parameters measured concurrently with net photosynthesis to investigate chloroplastic CO_2 concentration in leaves of Quercus ilex L. *Journal of Plant Physiology* **136,** 538–543.

Dreyer E, Le Roux X, Montpied P, Daudet F-A, Masson FA. 2001. Temperature response of leaf photosynthetic capacity in seedlings from seven temperate tree species. *Tree Physiology* **21,** 223–232.

Dubois JJB, Fiscus EL, Booker FL, Flowers MD, Reid CD. 2007. Optimizing the statistical estimation of the parameters of the Farquhar–von Caemmerer–Berry model of photosynthesis. *New Phytologist* **176,** 402–414.

Ellsworth DS, Reich PB. 1993. Canopy structure and vertical patterns of photosynthesis and related leaf traits in a deciduous forest. *Oecologia* **96,** 169–178.

Eschrich W, Burchardt R, Essiamah S. 1989. The induction of sun and shade leaves of the European beech (Fagus sylvatica L.): anatomical studies. *Trees—Structure and Function* **3,** 1–10.

Ethier GJ, Livingston NJ. 2004. On the need to incorporate sensitivity to CO_2 transfer conductance into the Farquhar–von Caemmerer–Berry leaf photosynthesis model. *Plant, Cell and Environment* **27,** 137–153.

Ethier GJ, Livingston NJ, Harrison DL, Black TA, Moran JA. 2006. Low stomatal and internal conductance to CO_2 versus Rubisco deactivation as determinants of the photosynthetic decline of ageing evergreen leaves. *Plant, Cell and Environment* **29,** 2168–2184.

Evans JR, Sharkey TD, Berry JA, Farquhar GD. 1986. Carbon isotope discrimination measured concurently with gas exchange to investigate CO_2 diffusion in leaves of higher plants. *Australian Journal of Plant Physiology* **13,** 281–292.

Farquhar GD, von Caemmerer S, Berry JA. 1980. A biochemical model of photosynthetic assimilation in leaves of C3 species. *Planta* **149,** 78–90.

Flexas J, Diaz-Espejo A, Galmes J, Kaldenhoff R, Medrano H, Ribas-Carbo M. 2007. Rapid variations of mesophyll conductance in response to changes in CO_2 concentration around leaves. *Plant, Cell and Environment* **30,** 1284–1298.

Flexas J, Ribas-Carbo M, Diaz-Espejo A, Galmes J, Medrano H. 2008. Mesophyll conductance to CO_2: current knowledge and future prospects. *Plant, Cell and Environment* **31,** 602–621.

Frak E, Le Roux X, Millard P, Dreyer E, Jaouen G, Saint-Joanis B, Wendler R. 2001. Changes in total leaf nitrogen and partitioning of leaf nitrogen drive photosynthetic acclimation to light in fully developed walnut leaves. *Plant, Cell and Environment* **24,** 1279–1288.

Hanba YT, Kogami H, Terashima I. 2002. The effect of growth irradiance on leaf anatomy and photosynthesis in Acer species differing in light demand. *Plant, Cell and Environment* **25,** 1021–1030.

Hothorn T, Bretz F, Westfall P, Heiberger RM. 2007. *multcomp: simultaneous inference for general linear hypotheses.* R package version 0.992-4.

Iio A, Fukasawa H, Nose Y, Kato S, Kakubari Y. 2005. Vertical, horizontal and azimuthal variations in leaf photosynthetic characteristics within a Fagus crenata crown in relation to light acclimation. *Tree Physiology* **25,** 533–544.

June T, Evans JR, Farquhar GD. 2004. A simple new equation for the reversible temperature dependence of photosynthetic electron transport: a study on soybean leaf. *Functional Plant Biology* **31,** 275–283.

Katahata SI, Naramoto M, Kakubari Y, Mukai Y. 2007. Seasonal changes in photosynthesis and nitrogen allocation in leaves of different ages in evergreen understory shrub *Daphniphyllum humile*. *Trees-Structure and Function* **21,** 619–629.

Kosugi Y, Matsuo N. 2006. Seasonal fluctuations and temperature dependence of leaf gas exchange parameters of co-occurring evergreen and deciduous trees in a temperate broad-leaved forest. *Tree Physiology* **26,** 1173–1184.

Leuning R. 1997. Scaling to a common temperature improves the correlation between the photosynthesis parameters J_{max} and V_{cmax}. *Journal of Experimental Botany* **48,** 345–347.

Lichtenthaler HK, Ac A, Marek MV, Kalina J, Urban O. 2007. Differences in pigment composition, photosynthetic rates and chlorophyll fluorescence images of sun and shade leaves of four tree species. *Plant Physiology and Biochemistry* **45,** 577–588.

Longdoz B, Gross P, Granier A. 2008. Multiple quality tests for analysing CO_2 fluxes in a beech temperate forest. *Biogeosciences* **5,** 719–729.

Loreto F, Harley PC, Dimarco G, Sharkey TD. 1992. Estimation of mesophyll conductance to CO_2 flux by 3 different methods. *Plant Physiology* **98,** 1437–1443.

Martinez DE, Guiamet JJ. 2004. Distortion of the SPAD 502 chlorophyll meter readings by changes in irradiance and leaf water status. *Agronomie* **24,** 41–46.

Meir P, Kruijt B, Broadmeadow M, Barbosa E, Kull O, Carswell FE, Nobre A, Jarvis PG. 2002. Acclimation of photosynthetic capacity to irradiance in tree canopies in relation to leaf nitrogen concentration and leaf mass per unit area. *Plant, Cell and Environment* **25,** 343–357.

Muraoka H, Koizumi H. 2005. Photosynthetic and structural characteristics of canopy and shrub trees in a cool-temperate deciduous broadleaved forest: implication to the ecosystem carbon gain. *Agricultural and Forest Meteorology* **134,** 39–59.

Murtaugh PA. 2007. Simplicity and complexity in ecological data analysis. *Ecology* **88,** 56–62.

Niinemets U. 1995. Distribution of foliar carbon and nitrogen across the canopy of Fagus sylvatica: adaptation to a vertical light gradient. *Acta Oecologica* **16,** 525–541.

Niinemets U, Cescatti A, Rodeghiero M, Tosens T. 2006. Complex adjustments of photosynthetic potentials and internal diffusion conductance to current and previous light availabilities and leaf age in Mediterranean evergreen species Quercus ilex. *Plant, Cell and Environment* **29,** 1159–1178.

Niinemets U, Tenhunen JD. 1997. A model separating leaf structural and physiological effects on carbon gain along light gradients for the shade-tolerant species Acer saccharum. *Plant, Cell and Environment* **20,** 845–866.

Piel C, Frak E, Le Roux X, Genty B. 2002. Effect of local irradiance on CO_2 transfer conductance of mesophyll in walnut. *Journal of Experimental Botany* **53,** 1–8.

Pons TL, Flexas J, von Caemmerer S, Evans JR, Genty B, Ribas-Carbo M, Brugnoli E. 2009. Estimating mesophyll conductance to CO_2: methodology, potential errors and recommendations. *Journal of Experimental Botany* **60,** 2217–2234.

R-Development-Core-Team. 2007. *R 2.6.0: a language and environment for statistical computing*. Vienna, Austria: R Foundation for Statistical Computing.

Richardson AD, Duigan SP, Berlyn GP. 2002. An evaluation of noninvasive methods to estimate foliar chlorophyll content. *New Phytologist* **153,** 185–194.

Roderick ML, Berry SL, Saunders AR, Noble IR. 1999. On the relationship between the composition, morphology and function of leaves. *Functional Ecology* **13,** 696–710.

Shipley B. 2000. *Cause and correlation in biology. A user's guide to path analysis, structural equations and causal inference*. Cambridge: Cambridge University Press.

Shipley B, Lechoweicz MJ, Wright I, Reich PB. 2006. Fundamental trade-offs generating the worldwide leaf economics spectrum. *Ecology* **87,** 535–541.

Tazoe Y, von Caemmerer S, Badger M, Evans JR. 2009. Light and CO_2 do not affect the mesophyll conductance to CO_2 diffusion in wheat leaves. *Journal of Experimental Botany* **60,** 2291–2301.

Terashima I, Miyazawa SI, Hanba YT. 2001. Why are sun leaves thicker than shade leaves? Consideration based on analyses of CO_2 diffusion in the leaf. *Journal of Plant Research* **114,** 93–105.

Uehlein N, Otto B, Hanson DT, Fischer M, McDowell N, Kaldenhoff R. 2008. Function of *Nicotiana tabacum* aquaporins as chloroplast gas pores challenges the concept of membrane CO_2 permeability. *The Plant Cell* **20,** 648–657.

Utsugi H, Tobita H, Maruyama Y, Ishizuka M. 2005. Spatial and seasonal variations in leaf mass per area and their relationship to leaf nitrogen in a secondary northern hardwood forest in Japan. *Phyton-Annales Rei Botanicae* **45,** 245–251.

van den Berg AK, Perkins TD. 2004. Evaluation of a portable chlorophyll meter to estimate chlorophyll and nitrogen contents in sugar maple (Acer saccharum Marsh.) leaves. *Forest Ecology and Management* **200,** 113–117.

von Caemmerer S. 2000. *Biochemical models of leaf photosynthesis*. Australia: CSIRO Publishing.

Wang Q, Iio A, Tenhunen J, Kakubari Y. 2008. Annual and seasonal variations in photosynthetic capacity of Fagus crenata along an elevation gradient in the Naeba Mountains, Japan. *Tree Physiology* **28,** 277–285.

Wang Q, Tenhunen J, Falge E, Bernhofer C, Granier A, Vesala T. 2003. Simulation and scaling of temporal variation in gross primary production for coniferous and deciduous temperate forests. *Global Change Biology* **10,** 37–51.

Warren C. 2006. Estimating the internal conductance to CO_2 movement. *Functional Plant Biology* **33,** 431–442.

Warren CR, Adams MA. 2006. Internal conductance does not scale with photosynthetic capacity: implications for carbon isotope discrimination and the economics of water and nitrogen use in photosynthesis. *Plant, Cell and Environment* **29,** 192–201.

Warren CR, Dreyer E. 2006. Temperature response of photosynthesis and internal conductance to CO_2: results from two independent approaches. *Journal of Experimental Botany* **57,** 3057–3067.

Wilson KB, Baldocchi DD, Hanson PJ. 2000. Spatial and seasonal variability of photosynthetic parameters and their relationship to leaf nitrogen in a deciduous forest. *Tree Physiology* **20,** 565–578.

Wilson KB, Baldocchi DD, Hanson PJ. 2001. Leaf age affects the seasonal pattern of photosynthetic capacity and net ecosystem exchange of carbon in a deciduous forest. *Plant, Cell and Environment* **24,** 571–583.

Yamori W, Noguchi K, Hanba YT, Terashima I. 2006. Effects of internal conductance on the temperature dependence of the photosynthetic rate in spinach leaves from contrasting growth temperatures. *Plant and Cell Physiology* **47,** 1069–1080.